

# Artificial intelligence and ANFIS reduced rule for equivalent parameter estimation of PV module on various weather conditions utilized for MPPT

Rati Wongsathan\* and Isaravuth Seedadan

Department of Electrical Engineering, Faculty of Engineering,  
North-Chiang Mai University 169 Hangdong Rd. Chiang Mai, Thailand 50230  
Tel. +66(53)819999, Fax.+66(53)819998 Email: isaratvuth@northcm.ac.th  
\*Correspondent author: rati@northcm.ac.th, rati1003@gmail.com

## Abstract

In order to facilitate the most appropriate and robust method for the overall efficiency of photovoltaic (PV), providing a more accurate optimization algorithm to extract the equivalent parameters of PV models prior to installation is necessary. In this paper, a numerical technique based on genetic algorithms (GAs) is performed to determine the equivalent parameters of PV solar module based on single diode model including with the photo current ( $I_{ph}$ ), the saturated diode current ( $I_s$ ), the series resistance ( $R_s$ ), the parallel resistance ( $R_{sh}$ ), and the ideality factor ( $n$ ). The measured I-V data from the experiment with the uncertainties arising from measurement noise in various weather conditions is adopted to extract these parameters by GA in order to overcome the local minima trap which occurs in the non-convex optimization problem. The preliminary solutions by GA extraction are used to train the estimation model including multi-layered perceptron neural network (MLPNN), radial basis function neural network (RBFNN), and adaptive neuro-fuzzy inference system (ANFIS) model for all weather conditions. The ANFIS model remarkably showed the best performance which preserves the RMSE lower than the rest for both the interpolation and extrapolation. However, the complexity caused by number of ANFIS model parameters and high computation time makes it unsuitable in the real practice. The ANFIS reduced model is then introduced and designed to select the significant rule node of ANFIS model by keeping an acceptable accuracy. The overall proposed model was used to determine the corresponding maximum power point (MPP) from the I-V characteristic obtained from the estimated parameter which generates the power difference as the input of the fuzzy logic controller (FLC) implementation based the maximum power point tracking (MPPT).

**Keywords:** *Multi-layered perceptron neural network, radial basis function neural networks, ANFIS, PV module, genetic algorithm*

## 1. Introduction

Solar energy is a promising, environment friendly and pollution free alternative source of electricity generation. Solar photovoltaic (PV) cell then becomes a key product for electrical power-generation technology, which can directly convert solar energy into direct current (dc). It suitably generates the electricity on-site in the remote and isolated areas without transmission losses. It has gained swift popularity from a small PV standalone site application to large PV grid connected system [1]. Thailand has been using this technology since 1976 and has continuously made developments in various field applications e.g. battery charger, repeater signal station, water pumping, illumination, etc. [2]. The biggest amorphous thin film solar power plant in the world is also located in Lop Buri province of central Thailand which can produce electrical power up to 73 MW. During 2012-2021, according to the alternative energy development plan Thailand will raise its production of renewable electrical power up to 6,000 MW (Ministry of energy, Thailand, 2012). However, due to the high fixed and maintenance cost, this technology is not more attractive for the household. Further, lack of the basic knowledge on power efficiency conversion of PV system makes the power per capita higher than the other conventional resources. Nowadays, all costs have been reduced due to the modern semiconductor fabrication. The efficiency of PV is the only issue for consideration.

PV cell is basically a p-n junction fabricated in a thin wafer or layer of semiconductors. The electromagnetic radiation of solar energy can be directly converted to electricity by PV cell through

photoelectric effect. In application, the solar module consists of multi solar cells in series connected to increase power and voltage above that from the single solar cell and has the same I-V characteristic except with the change in the magnitude of current and voltage. The current-voltage (I-V) characteristic of PV cell exhibits a non-linear relationship and is weather dependent. An exact equivalent circuit and its associated mathematical model are essential for providing accurate I-V characteristic of the PV cell. The convenient and most common way in most simulation studies used in PV cell model is the single diode lumped equivalent circuit model with single exponential term [3] which is illustrated in Fig. 1.

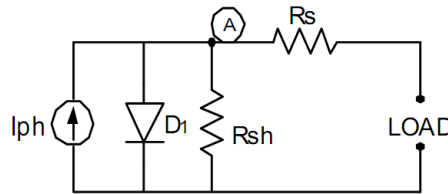


Figure 1 The equivalent PV cell circuit based on single diode model.

It combines with five unknown parameters including the photo-current ( $I_{ph}$ ), diode saturation current ( $I_{sd}$ ), series resistance ( $R_s$ ), parallel or shunt resistance ( $R_{sh}$ ), and the ideality factor of diode ( $n$ ). Physically, at short circuit state the photo-current generated by a solar cell under illumination is dependent on the incident light while diode saturation current is the flowing current through the diode. The series resistance arises from the resistance of the cell material to current flow, particularly through the front surface to the contacts and from resistive contacts. The shunt resistance arises from leakage of current through the cell, around the edge of the device and between contacts of different polarity. The ideality factor of diode accounts for the differential mechanism responsible for moving carriers across the p-n junction. For the other PV model with four unknown parameters which infers the shunt resistance is infinite and with three unknown parameters which assumes that series resistance is also zero are represented in reference [4] and [5] respectively. Whereas, the double diode equivalent circuit models [6] have six unknown parameters with two exponential terms. Both single and double diode models require the knowledge of all unknown parameters, which is usually not provided by the manufacturers.

To obtain the accuracy equivalent circuit model, the equivalent circuit parameters extraction approach is mostly required. Since the I-V relationship is a nonlinear and implicit transcendental expression then it has not the explicit analytical solution. The analytical methods give exact solution by means of algebraic equations. However, it is also time consuming to discover its exact analytical solution due to unavailable data for the extraction of required parameters. Some numerical methods do exist which obtain those parameters from the manufacturer's data, are iterative and non-straight forward. The solution always depends on the initial value which may not converge to the final result for every case making it unreliable. Due to loss of some information and non-provision of data from the manufacturers, the parameter extraction is still a difficult task that requires both experimental data and calculation procedures. Furthermore, parameters are naturally changed according to variations of the irradiance and cell temperature at each operating point. The next challenging task is to estimate the equivalent circuit model through the equivalent parameters depending on weather conditions. Use of accurate PV model represented with affecting parameters is also necessary for proper performance evaluation and power control. In order to track the maximum power point (MPP) of the PV cell by various control techniques, the accuracy of method depends on the knowledge of these PV cell parameters which are usually extracted from the experimental data.

The main contribution of this work is searching for the accurate equivalent circuit based single diode model of PV module under wide range of weather conditions in order to specify the maximum power at the operating point. This point is used to be the reference of the MPPT control algorithm. The equivalent parameters of the PV module model are only extracted from the measured I-V data collected from the experimental laboratory at irradiance and temperature set up conditions. Genetic algorithm (GA) is selected as the tool to extract the parameters at several operating points and generated the initial solutions for the estimation model. The accuracy of the estimation model has been obtained from the artificial intelligence methods including: feed forward multilayer perceptron neural networks model

(MLPNN), Radial Basis Function neural networks model (RBFNN), and ANFIS model. Further, the best performance model employs to estimate the voltages and currents corresponding to maximum power point of PV modules. At the beginning, implementation of these proposed models is initially demonstrated by the simple and conventional maximum power point tracking (MPPT) control namely perturb and observe (P&O) method and incremental conductance (IC) method. In this work, the MATLAB code was developed for GA and ANFIS instead of using MATLAB global optimization toolbox for the design purpose.

In the following sections, available methods for parameter extraction in PV are reviewed and examined. The choice of the best method adaptable existing data and constraint due to the available data offered from the manufactures. The PV module model and nonlinear  $I$ - $V$  characteristic equation depends on both irradiance and temperature is shortly described in section 3.1. The parameter extraction procedure by GA is stepwise detailed in section 3.2. The estimation models i.e. MLPNN, RBFNN, and ANFIS model are simultaneously represented with the optimized structure model by the designed experiment in section 3.3, 3.4, and 3.5 respectively. The interpolation and extrapolation results from all estimation models are shown and discussed in section 4.1. The reduce rule concept for ANFIS model by using GA is introduced in section 4.2. An MPPT controller implemented based on the best estimation model is also demonstrated in section 4.3. Conclusions have been drawn in the last section.

## 2. Literature review

The parameter estimation of PV cell is critical for determining the device's output performance and efficiency. Evaluation of the parameter has been the subject of investigation by several methods, e.g. analytical method, numerical analysis or iterative method and evolutionary computation method. Analytical method is the commonly used simple approach in the parameter extraction by concerning of mathematical equations. By introducing several assumptions, e.g. parameter  $n$  is assumed to be within the range [1, 2] according to moving carriers across the p-n junction process case,  $I_{ph}$  is assumed to be equal to the short circuit current, and etc., the complex non-linear relationships that define the behavior of a solar cell can be reduced to analytically solvable equations. However, it is a difficult task and laborious. Analytical method with simplification and approximation was firstly used in reference [7] which has been applied co-content function based on Lambert's  $W$  function which allows the eq.(1) in section 3.1 to be explicitly solved for the load voltage as a function of the load current  $I = I(V)$  and for the load voltage as a function of the load current  $V = V(I)$ . Lambert's  $W$  function is the solution  $W(x)$  of the equation  $x = W(x)\exp(W(x))$ . However, equating the derivative of the voltage and current product to zero does not allow analytical solution for either the maximum voltage or current which means impossible for maximum power. Reference [8] used the Lambert's  $W$  function to present a PV array model in diverse environmental condition and pointed out that it significantly reduces calculation time. Optimized method based on polynomial curve fitting and Lambert's  $W$  function for extraction of parameters from the current-voltage ( $I$ - $V$ ) characteristics of commercial silicon solar cell is proposed by [9]. Artificial neural networks together with the Lambert's  $W$  function were employed for determination the  $I$ - $V$  and  $P$ - $V$  curves of silicon and plastic solar cells and module [10]. However, due to implicit nature and nonlinearity of PV cell or module characteristics, it is difficult to express the analytical solution of all unknown parameters. They also have some limitations and could not give exact solutions when the functions are not given then numerical methods were preferred.

On the other hand, various numerical analysis methods have been applied to determine model parameters of solar cells such as root-finding in reference [11] and [12], or global optimization in reference [13] and [14], both of which involve iteration to solve for current or voltage and simultaneously adjusts parameter values to minimize an error metric. A modified non-linear least error squares estimation approach based on Newton's method is used to determine solar cell parameters in reference [15]. However, these approaches suffer from its high dependency on the initial values selecting. It is hard to further reduce the errors of the estimated values and required the  $I$ - $V$  curve features or semiconductor parameters that are unavailable in the datasheet.

## 3. Research model and methods

### 3.1 PV module model

Recently, PV parameter estimation is assumed as a multidimensional optimization problem. Several computational intelligence methods, such as Genetic algorithm (GA) in reference [16], Particle Swarm Optimization (PSO) in reference [17], Chaos Particle Swarm Optimization (PSO) in reference [18], Firefly in reference [19], Pattern Search (PS) in reference [20], Simulated annealing (SA) in reference [21], and Fuzzy logic in reference [22] were proposed to extract the parameters by minimizing the root mean square error RMSE as the objective function in the literatures which were reported to produce better results than analytical method. These methods have received remarkable attention as a derivative free, robust and often involve a small number of parameter tunings.

In summary, the algorithm for determining model parameters of solar cells, can be divided into two groups i.e. first method uses the selected parts of the  $I$ - $V$  characteristic e.g. the open-circuit and short circuit coordinates, the maximum power points and slopes at strategic portions for different level of irradiance and temperature and second method takes all the experimental data in consideration (curve fitting). First method is often much faster and simpler but less accurate in comparison with curve fitting. In curve fitting procedure, traditional deterministic optimization algorithms lead to local minima solution.

The estimation model takes an important role for interpolation and extrapolation at variety of weather conditions for giving extracted parameters data. Radial Basis Function Neural Networks (RBFNN) was used to estimate the electrical characteristic curve of PV modules from various environmental conditions [23]. A hybrid Neuro-fuzzy based on an AI technique which combines the advantages of NNs and fuzzy logic is applied for PV parameter estimation [24]. Literature survey revealed that these methods have both advantages and disadvantages by their aspects which have not significantly different in resulted solutions.

The single diode model is adopted to fit the equivalent PV module circuit with simple, efficient and sufficiently acceptable for optimization process and system design tasks. Although, the output power of a solar module generally depends on the electrical characteristic of the poor cell in the module [16]. In this work, equivalent circuit parameters of all cells are assumed to form a similar electrical characteristics and the property variation from cell to cell can be neglected. Further, the loss occurring inside the cell due to charge carriers' accumulation by the electrodes covering the semiconductor is also neglected. Then, the single diode model can also be applied to formulate a solar module by these assumptions.

Naturally, PV system exhibits a nonlinear current-voltage ( $I$ - $V$ ) and power-voltage ( $P$ - $V$ ) characteristics which are shown in Fig. 2. An equivalent circuit of PV module with composed of  $N_s$  cells in series connection and referenced in Fig.1 produced the non-linear load current-voltage ( $I_L$ - $V_L$ ) characteristics when it is illuminated. PV cell in module generates current and link to a parallel diode with an  $I$ - $V$  characteristic which is mathematically defined by Shockley in the following simple equation as

$$I_L = I_{ph} - I_{sd} \left[ \exp \frac{q(V_L / N_s + I_L R_s)}{n K_B T} - 1 \right] - \left[ \frac{V_L / N_s + I_L R_s}{R_{sh}} \right] \quad (1)$$

where  $K_B$  is Boltzmann's constant ( $1.38 \times 10^{-23}$  J/K),  $q$  is the electron charge ( $1.60 \times 10^{-19}$  C), and  $T$  is the cell temperature in Kelvin (K).  $I_{pv}$  is a function of incident solar irradiance and cell temperature which is given by

$$I_{ph} = [I_{sc} + K_I(T - T_0)] \frac{G}{G_0}, \quad (2)$$

where  $I_{sc}$  is the short circuit current at STC,  $T_0$  and  $G_0$  are the reference temperature and irradiance at STC in K and  $W/m^2$  respectively,  $K_I$  is the short circuit current temperature coefficient. The diode saturation current of the PV module varies with temperature according to the following equation,

$$I_{sd} = I_{sd,0} \left[ \frac{T}{T_0} \right]^3 \exp \left[ \frac{q E_g}{n k_B} \left( \frac{1}{T_0} - \frac{1}{T} \right) \right], \quad (3)$$

where  $I_{sd,0}$  is the saturation current at  $T_0$ ,  $E_g$  is the band gap energy of the semiconductor.

In classical curve fitting method, the error criterion is based on the average of sum of the squared distances between the experimental data,  $I_j$  and predicted data,  $\hat{I}_j(V_j, \theta)$  which is expressed as,

$$S(\theta) = \frac{1}{M} \sum_{j=1}^M [I_j - \hat{I}_j(V_j, \theta)]^2, \quad (4)$$

where  $\theta = \{I_{ph}, I_{sd}, R_s, R_{sh}, n\}$ ,  $I_i$  and  $V_i$  are respectively the measured current and voltage at the  $j^{th}$  point of  $M$  data points. The  $\hat{I}_j(V_j, \theta)$  can be simplify computed by substituting  $I_j$  and  $V_j$  in eq. (1),

$$\hat{I}_j(V_j, \theta) = I_{ph} - I_{sd} \left[ \exp \frac{q(V_j / N_s + I_j R_s)}{n K_B T} - 1 \right] - \left[ \frac{V_j / N_s + I_j R_s}{R_{sh}} \right] \quad (5)$$

According to the fact that the objective function in eq. (5) of the parameter extraction process tends to be a multi-dimensions. To solve the nonlinear in eq. (5) by analytical approach under variety weather conditions of  $G$  and  $T$ , at least 5 points i.e. the current and voltage at the maximum power point (MPP), short-circuit current ( $I_{sc}$ ), open-circuit voltage ( $V_{oc}$ ), and slopes of the  $I$ - $V$  characteristic at the axis intersection are required to formulate 5 equations according to 5 unknown parameters. It is quite difficult to determine the parameters for each weather condition in running simulation studies or online PV system application [21]. In numerical approach, all points of data along  $I$ - $V$  characteristic are utilized based on certain mathematical algorithm. The estimation result is obtained more accurate than the analytical approach [15]. Regardless of gradient and initial condition information using by numerical approach, evolutionary algorithm such as genetic algorithm (GA) can be very effective. For this reason, in this work, all 5 unknown parameters are preliminarily estimated off line by genetic algorithm (GA) at several weather conditions other than the STC and subsequently performed an interpolation and extrapolation by AI methods which are mentioned in the next section respectively.

In the test, a polycrystalline silicon commercial (SHARP type ND-130T1J) with 36 cells ( $N_s = 36$ ) series connected without the information of the equivalent circuit parameter is the case study. The technical specifications of this sample PV module are collected in Table 1.

Table 1 Technical specifications of a polycrystalline silicon commercial type SHARP type ND-130T1J.

PV module parameters	Single cell	Series in module
Rated power, W	4.06	130
Voltage at MPP ( $V_{mp}$ )	0.54	17.4
Current at MPP ( $I_{mp}$ )	7.48	7.48
$V_{oc}$	0.687	22.0
$I_{sc}$	8.09	8.09

### 3.2 Parameter extraction using GA

In this section, equivalent PV module circuit parameters based on the single diode model is going to be evaluated by GA. The  $I$ - $V$  data is measured for various weather conditions (values of  $G$  &  $T$ ). The measurement noise is important consideration since it obscures parameter extraction, especially if the method is based on using few experimental points such as the conventional analytical method mentioned in section 3.1. In this work, the high measurement noise exists from various ways i.e. the human, fast variation of weather condition, accuracy of instrument, deficiency of PV module etc. To reduce the possible uncertainties arising from measurement noise, the robust technique as GA based on taking many data points is selected to extract the parameter of equivalent PV module circuit.

GA is an evolutionary algorithm based on natural selection of the fittest survival [26]. It operates on a coded parameter set of the solution under the cost function with derivative free. It finally employs pseudo-probabilistic rules and not deterministic ones. The detail stepwise procedure of GA implementation for PV module parameter extraction is described below:

Step 1, the 5 parameters including  $I_{ph}$ ,  $I_{sd}$ ,  $R_s$ ,  $R_{sh}$ , and  $n$  were represented by a chromosome which is encoded with  $N_{bit}$  bits of binary coding.

Step 2, the initial population ( $N_{pop}$ ) are randomly generated. Each individual possesses vector entries with certain length of gene.

Step 3, the binary value of each gene is normalized within the range  $[Q_{min}, Q_{max}]$  by linear mapping function:

$$gene(i) = Q_{i,min} + \frac{(Q_{i,max} - Q_{i,min}) \times y(i)}{2^{N_{Bit}} - 1} . \quad (6)$$

Here  $y(i)$  is binary value of each gene. In this paper,  $I_{pv}$ ,  $I_{sd}$ ,  $R_s$ ,  $R_{sh}$ , and  $n$  are normalized within the searching range given as  $[1, 10]$ ,  $[1 \times 10^{-6}, 100 \times 10^{-6}]$ ,  $[0.05, 5]$ ,  $[100, 2000]$  and  $[0.5, 5]$  respectively.

Step 4, each chromosome is determined the fitness of individual by evaluation function or objective function which is a function of  $S(\theta)$  in eq. (4) and defined as,

$$f(\theta) = \frac{100}{\sqrt{S(\theta) + 1}} . \quad (7)$$

To challenge the search of GA, eq. (4) exhibits a nonlinear form with many local minimum instead of the quadratic form.

Step 5 (Selection), the parent chromosomes based on their fitness value are chosen by two methods. First, the elitism method is used to retain the best chromosome that passes through the reproduction step. Second, the roulette wheel method is applied to the remaining populations by assigning a higher probability of selection to individuals with higher fitness.

Step 6 (Reproduction), this procedure take two selected chromosomes from a current generation (parent) and cross them to obtain two individuals for the new generation. Reproduction option will determine how the GAs produces the children for the next generation. Two types of reproduction in this paper are crossover and mutation.

Step 7, the new generation from step 6 is brought to replace the current population. The iteration is then updated by 1:  $Gen = Gen + 1$ . Steps 2-6 are repeated in the new generation until convergence is achieved.

The algorithm breaks if it meets any one of three stopping criteria i. e. maximum number of generation, fitness limit and time limit. The parameter setting is as follows: population size equals to 50, maximum generation process set to 3000, multiple point crossover type with crossover rate equals to 0.85, multiple point mutation type with mutation rate equals to 0.15, and roulette wheel selection with the elitism rate set to 10%. For flexibility and objective design, the GAs programming is made them up without using Genetic Algorithm and Direct Search Toolbox of Matlab. From our proposed GA, the 5 parameters ( $I_{ph}$ ,  $I_{sd}$ ,  $R_s$ ,  $R_{sh}$ , and  $n$ ) are determined from the  $I$ - $V$  experimental data with various weather conditions. At the STC, the PV module circuit parameters extracted by GA searching are found that  $I_{ph} = 8.01$  A,  $I_s = 8.77 \mu\text{A}$ ,  $R_s = 0.016 \Omega$ ,  $R_{sh} = 690.72 \Omega$  and  $n = 1.877$ . The comparison simulation play-back resulting by using this GA parameters extracted as described above together with the measured data  $I$ - $V$  obtained from the PV module case are illustrated in Fig. 2.

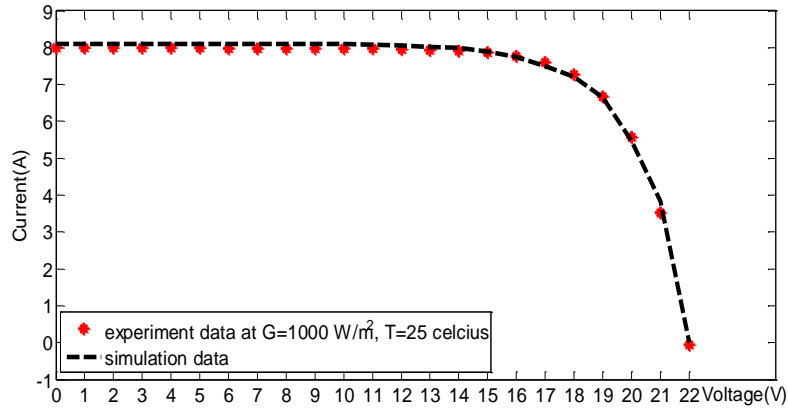


Figure 2 The comparison results of I-V characteristic at STC between the measured data and the simulation through parameter extracted by GA.

For the other weather conditions (values of  $G$  and  $T$ ), the parameter extraction results by GA are shown in Table 2 (provided at the end of the paper). The  $I$ - $V$  characteristics of PV module with those parameters for the various weather conditions are shown for example in Fig. 3 (a) and (b).

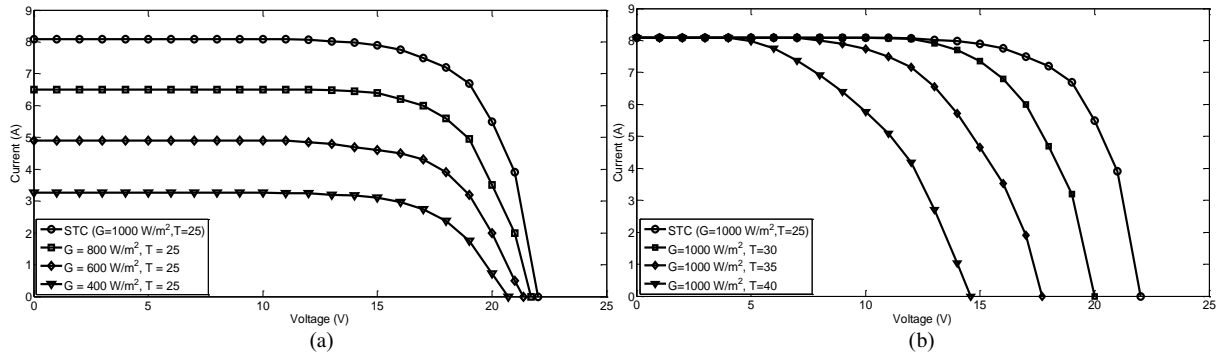


Figure 3 The  $I$ - $V$  characteristic of PV module resulted from parameter extracted by GA for the conditions (a) constant  $T = 25^\circ\text{C}$  and  $G$  is varied by 1000, 800, 600, and 400  $\text{W}/\text{m}^2$ , and (b) constant  $G = 1000 \text{ W}/\text{m}^2$  and  $T$  is varied by 25, 30, 35, and 40  $^\circ\text{C}$ .

For the case of temperature constant in Fig. 3(a), the irradiance are varied from 1000 to 400  $\text{W}/\text{m}^2$  by the decreasing step size of 200, the characteristic of  $I$ - $V$  are simultaneously changed. The  $I_{sc}$  is decreased with corresponding decrease in irradiance, while  $V_{oc}$  is changed little. It is shown that the short circuit current has linear relation with solar irradiance while the open circuit has a non-linear relation. In Fig. 3(b), while keeping irradiance constant when  $T$  is varied from 25 to 30  $^\circ\text{C}$  by the increasing step size of 5, the short circuit current has slightly changed while the open circuit voltage has linearly varied with temperature.

The preliminary parameters at various weather conditions determined by GA extraction as described above will be used as the training and testing data for the estimation model i.e. MLPNN, RBFNN, and ANFIS. The overall procedure of these estimation models are presented in section 3.3-3.5, respectively.

### 3.3 PV module parameter estimation by MLPNN

An NNs is an imitation of simulating human brain cells using a computational model. It is regarded as multivariate, nonlinear and nonparametric method which can well reveal the correlation of nonlinear relation between input and output variables. By learning the mapping input-output data, ANN model can be built without explicit formulating the possible relationship that exists between variables. In this work, Multi-layer perceptron neural network (MLPNN) a kind of feed-forward neural network was selected to purpose as the mapping function model. It typically consists of a three-layers in the structure which consists of an input layer, a hidden layer with  $n$  hidden node and nonlinear function commonly a hyperbolic tangent function  $g(\cdot)$ , and an output layer with linearly transfer function  $f(\cdot)$ , and is shown in the dash box of Fig. 4.

The output of MLPNN is referred as the estimation parameter of PV module,  $\theta = \{I_{pv}, I_{sd}, R_s, R_{sh}, n\}$ , at the weather condition  $(G, T)$  which is treated as the input of the NNs. The weighted summation of each hidden layer neuron's output can be mathematically expressed in vector form as

$$\theta = f \left( \mathbf{W}^{(2)} \times g \left( \mathbf{W}^{(1)} \times \mathbf{PM} + \mathbf{b}^{(1)} \right) + \mathbf{b}^{(2)} \right), \quad (8)$$

and  $\mathbf{W}^{(1)}$  and  $\mathbf{b}^{(1)}$  is weight matrix and bias vector between input and hidden layer respectively,  $\mathbf{W}^{(2)}$  and  $\mathbf{b}^{(2)}$  is the weight vector and bias vector between hidden and output layers respectively. The parameter of NNs i.e. weight and bias are searched by the well-known learning, back-propagation (BP) algorithm.

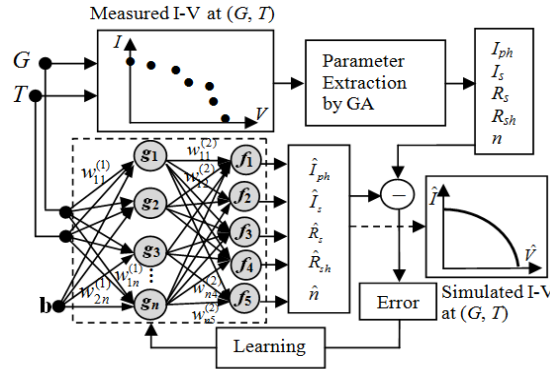


Figure 4 Parameters estimation by MLPNN model with using train and test data from prior parameter extraction by GA.

For MLPNN structure, the optimized hidden node from computer simulation is determined by considering the average of root mean square of error (RMSE) between the estimated and test parameters. The test data are divided into 2 samples i.e. interpolate data and extrapolate data which is used to validate the estimation model for within and extending to the train values respectively. The RMSE results from interpolation and extrapolation are shown in Fig. 5. It can be seen that, when RMSE kept constant at the hidden node number equals to 5 for all parameters then the optimized hidden node is also 5. The MLPNN estimation model is denoted as MLPNN(2, 5, 5) which 2, 5, and 5 refers to the number of input, hidden, and output nodes respectively. From this optimized structure, the number of parameter including weight and bias values is totally  $(2 \times 5 + 5 \times 5) + (5 + 5) = 45$  parameters which are adjusted by BP algorithm. Additionally, the RMSE of the extrapolation method resulted higher than the interpolation method about 40% by average.

RBFNN is another kind of the feed forward NNs which is introduced to compare the performance with MLPNN for the PV module parameters estimation. Both are considered as the universal approximator. The advantages and disadvantages of these two types of NNs depend on the nature of the problem. For function approximation problem, reference [27] suggested that RBFNN are specially recommended for surface with regular minima and maxima while MLPNN are preferred as a general model with the unusual surface. RBFNN model for PV module estimation detail is described in the next section.

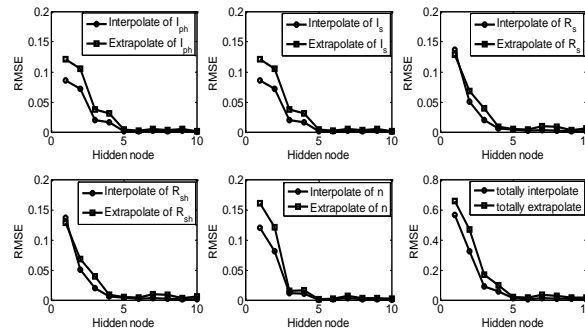


Figure 5 Relation between RMSE and hidden node for PV module parameters by MLPNN model.



### 3.4 PV module parameter estimation by RBFNN

MLPNN which may have more than three layers architectures making it quite slow learning and usually trapped in the local minima than RBFNN. The compact topology and faster learning speed made RBFNN attractive and considerable. The RBFNN is a fixed three-layer feed-forward neural network which consists of an input layer, a hidden layer with radial activation function neurons commonly normally Gaussian function which remaps the input data in order to make them linearly separable, and the output layer with linear neurons. The architecture of RBFNN of PV module parameter estimation is shown in the dash box of Fig. 6.

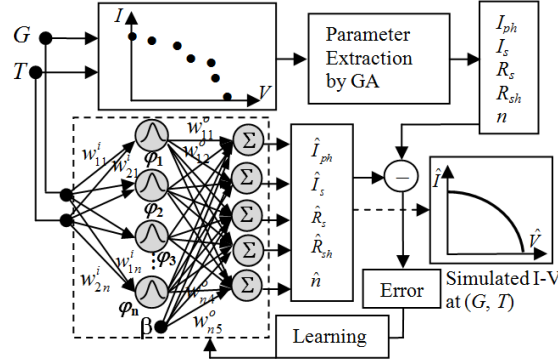


Figure 6 Parameters estimation by RBFNN model with using train and test data from prior parameter extraction by GA.

At the input of hidden unit, the input vector of  $x = [G \ T]'$ , where ' denotes the transpose, is weighted by input weights,  $w^i$  to produce  $s_k$  as

$$s_k = [Gw_{1,k}^i, Tw_{2,k}^i], \quad (9)$$

where  $k$  is the index of the hidden units and  $w_{1j}^i$  and  $w_{2j}^i$  are the weight between input node in the hidden layer and the  $k^{th}$  node in the hidden layer. The output of the hidden unit  $k$ ,  $\phi_k(s_k)$  is calculated by

$$\phi_k(s_k) = \exp(-\|s_k - c_i\|^2 / 2\alpha_i^2), \quad (10)$$

where  $\alpha_i$  and  $c_i$  is the spread and center of  $i^{th}$  node in hidden layer.

The output of RBFNN,  $\theta = \{I_{ph}, I_s, R_s, R_{sh}, n\}$ , is the weighted summation of each hidden layer neuron's output which can be expressed as

$$\theta_j = \sum_{k=1}^n w_{k,j}^o \phi_k(s_k) + \beta_j, \quad (11)$$

where  $n$  is the number of node in the hidden layer and indexed by  $k$ ,  $j$  is the index of the output node by  $j \in \{1, 2, \dots, 5\}$  corresponds with 5 parameters of PV module,  $w_{kj}^o$  is the weight between  $k^{th}$  node in the hidden layer and  $j^{th}$  node in the output layer, and  $\beta_j$  is the bias of  $j^{th}$  node in output layer.

From eq. (7)-(9), there are four types of parameters including input weight matrix ( $w^i$ ), output weight matrix ( $w^o$ ), center vector ( $c$ ), and spread vector ( $\alpha$ ). To simplify the searching plane of RBFNN, all parameters in the input weight matrix were set to 1. For a rapid convergence of solution, the spread parameter of the Gaussian function was properly selected by the experiment. The larger spread parameter the smoother function approximation, a lot of hidden node will be required to fit the fast changing function. While, the smaller spread parameter means many hidden nodes will be required to fit a smooth function and the network may not generalize well. The designed spread parameter by using RMSE performance in Fig.7 have found that the optimized spread parameter is 1 since the RMSE did not improve by increasing the spread parameter more than its value.

Then, the spread vector were set to 1 and eq. (11) is rewritten as

$$\theta_j = \sum_{k=1}^n w_{k,j}^o \exp(-\|x - c_i\|^2 / 2), + \beta_j \quad (12)$$

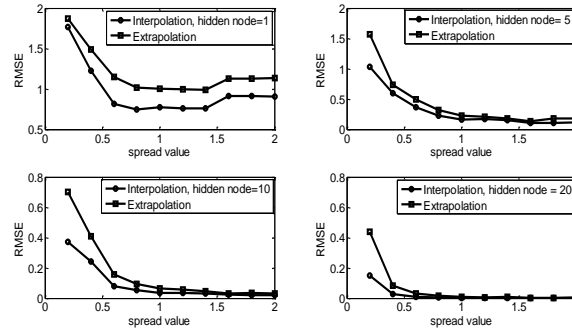


Figure 7. Relation between RMSE and spread parameter for radial basis node cases.

The rest of RBFNN structure parameter was adjusted by the learning algorithm which is divided into two stages. In the first stage, the unsupervised learning process such as K-mean algorithm [28], orthogonal least squares (OLS) algorithm [29], etc. are used to solve the center and spread or variance of Gaussian function. In the second stage, the supervised learning process such as gradient descent algorithm, least square algorithm, etc. are used to adjust the input and output weight matrix. In the parameter estimation of PV module, the number of input node is defined by 2 for  $G$  and  $T$ , the number of output node is defined by 5 for PV module parameters, and number of hidden node is determined and selected by the experimental design.

For RBFNN structure, the optimized hidden node from computer simulation is determined by considering the RMSE between the estimated and test parameters. The same data test set used in MLPNN is repeatedly applied to RBFNN model. The RMSE results are graphically shown in Fig. 8.

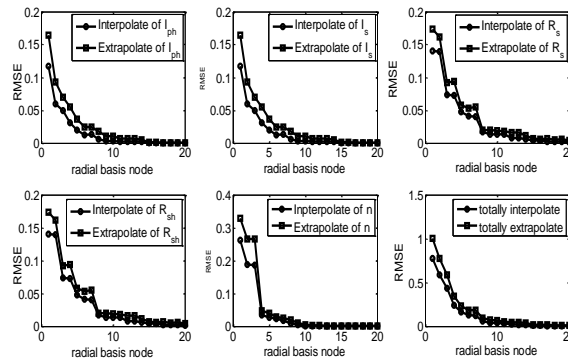


Figure 8. Relation between RMSE and RBF node for parameter estimation of RBFNN model.

It can be seen that RMSE is kept constant at radial basis node equals to 15 for all parameters then the RBFNN is denoted by RBFNN(2, 15, 5) which 2, 15, and 5 refers to the number of input, hidden, and output nodes respectively. From this optimized model, the number of adjusted parameter including output weight, bias, and center values of the RBF is in total  $(15 \times 5) + (1 \times 5) + (1 \times 15) = 95$  parameters. Additionally, the RMSE of the extrapolation method is higher than the interpolation method about 37% by average.

### 3.5 PV module parameter estimation by ANFIS model

ANFIS is used to apply in many complicated problems because it combines the advantages of NNs and the linguistic interpretability of a FIS. In this work, ANFIS is adopted to estimate the PV module parameter by using 2 inputs of  $G$  and  $T$  which has  $N_G$  and  $N_T$  membership functions and one output for each five equivalent parameters results in five ANFIS estimation models. As shown in Fig. 9, the ANFIS model includes 5 layers in which nodes of the same layer have similar functions.

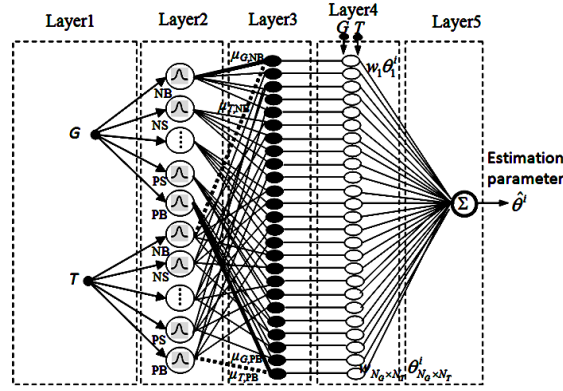


Figure 9. ANFIS architecture for estimation PV module parameter.

In layer 1, input  $G$  and  $T$  are normalized to the range  $[0, 1]$ .

In layer 2, adaptive node with the Gaussian function computes the membership function ( $\mu$ ) of fuzzy set  $G = \{NB, NS, \dots, PS, PB\}$  and  $T = \{NB, NS, \dots, PS, PB\}$  with  $N_G$  and  $N_T$  membership functions respectively which can be expressed as  $\mu_{G_x}$  and  $\mu_{T_x}$  where  $x \in \{NB, NS, \dots, PS, PB\}$ ,

In layer 3, the constructed rule base with 2 input fuzzy sets,  $N_G \times N_T$  if-then rules is shown in the example below for a first-order Sugeno fuzzy model. In evaluating the rule premise, the product for  $T$ -norm (logical *and*) is chosen and resulted the weight values as

$$w_j = \mu_{G_x}(G) \times \mu_{T_x}(T), \quad j = 1, 2, \dots, N_G \times N_T, \quad (13)$$

*Rule1:* if  $G$  is  $NB$  and  $T$  is  $NB$ , then  $\theta_1^i = p_1^i G + q_1^i T + r_1^i$

*Rule2:* if  $G$  is  $NB$  and  $T$  is  $NS$ , then  $\theta_2^i = p_2^i G + q_2^i T + r_2^i$

...

*Rule  $N_G \times N_T$ :* if  $G$  is  $PB$  and  $T$  is  $PB$ , then  $\theta_{N_G \times N_T}^i = p_{N_G \times N_T}^i G + q_{N_G \times N_T}^i T + r_{N_G \times N_T}^i$

In layer 4, the weighted rule consequences correspondence with the weight values and posed them to the layer 5 for evaluating the implication.

In layer 5, output parameter is averagely calculated by

$$\theta^i = \sum_{j=1}^{N_G \times N_T} w_j \theta_j^i(G, T) / \sum_{j=1}^{N_G \times N_T} w_j \quad (14)$$

For ANFIS model in Fig. 9 as an example model, the parameter including the center ( $c$ ) and the standard deviation ( $\sigma$ ) of all Gaussian membership functions of each input  $G$  and  $T$ , and the consequences parameter ( $p$ ,  $q$ , and  $r$ ) of first order in Sugeno type of fuzzy according with the  $N_G \times N_T$  rules yields  $2 \times N_G + 2 \times N_T + 3 \times N_G \times N_T$  parameters which are normally adjusted through a hybrid learning rule combining the BP gradient descent and a least-squares method. For ANFIS structures optimization, the experimental design was set to observe the RMSE according to number of membership function of each input  $G$  and  $T$ . The results of 35 ( $N_G, N_T$ ) are combinations from (1, 2), (1, 3), ..., (6, 6) presented in the Fig. 10.

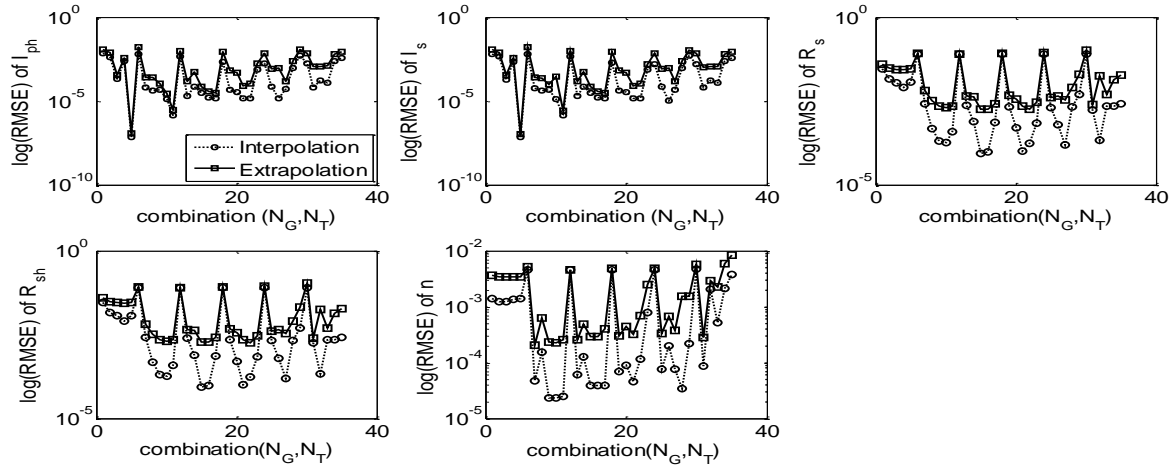


Figure 10. Relation of RMSE on logarithm scale and the combination between membership function of  $G$  and  $T$  of ANFIS model.

The most suitable choice of the combination  $(N_G, N_T)$  in order to keep lowest RMSE for each parameter  $I_{ph}$ ,  $I_s$ ,  $R_s$ ,  $R_{sh}$ , and  $n$  is (1, 6), (1, 6), (3, 4), (3, 4) and (2, 5) respectively.

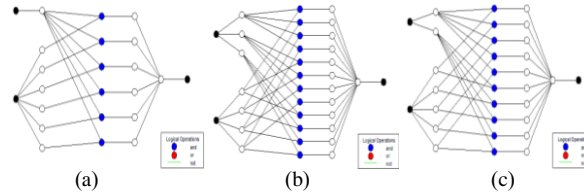


Figure 11. Equivalent parameter estimation of PV module by using (a) ANFIS (1, 6) for parameter  $I_{pv}$  and  $I_s$ , (b) ANFIS(3, 4) for parameter  $R_s$  and  $R_{sh}$ , and (c) ANFIS (2, 5) for parameter  $n$ .

The parameter of ANFIS structure corresponds with the selected  $(N_G, N_T)$  of each parameter is 32, 32, 50, 50, and 50 respectively, and yields a total of 212 parameters for all parameters. ANFIS structure from the experimental designed above which denoted ANFIS (1, 6), ANFIS(3, 4) and ANFIS(2, 5) were shown in Fig. 11 (a) for parameter  $I_{ph}$  and  $I_s$ , (b) for parameter  $R_s$  and  $R_{sh}$  and (c) for parameter  $n$ . The parameter of the Gaussian function used as the fuzzy set of input  $G$  ( $X_{i,G}$ ) and  $T$  ( $X_{i,T}$ ).

## 4. Empirical results and analysis

### 4.1 Parameter estimation results

The estimation model of MLPNN and RBFNN with 2 inputs  $G$  and  $T$  and 5 outputs estimated parameter of equivalent circuit PV module by the design experimental in the last section have resulted for one hidden layer with 5 hidden nodes and 15 radial basis function respectively and denoted as MLPNN(2,5,5) and RBFNN(2,15,5). While ANFIS model has 5 distinct models which correspond to 5 equivalent circuit parameters. For parameter  $I_{ph}$  and  $I_s$ , ANFIS model has the number of linguistic fuzzy set of input  $G$  and  $T$  as 1 and 6 which generated 6 rule nodes and denoted as ANFIS([1,6],6,1). For parameter  $R_s$  and  $R_{sh}$ , ANFIS model has the number of linguistic fuzzy set of input  $G$  and  $T$  as 3 and 4 which generated 12 rule nodes and denoted as ANFIS([3,4],12,1). For parameter  $n$ , ANFIS model has the number of linguistic fuzzy set of input  $G$  and  $T$  as 2 and 5 which generated 10 rule nodes and denoted as ANFIS([2,5],10,1). The estimation for all parameter by these selected estimation models for RMSE of interpolation and extrapolation are shown in Fig.12 (a) and (b) respectively.

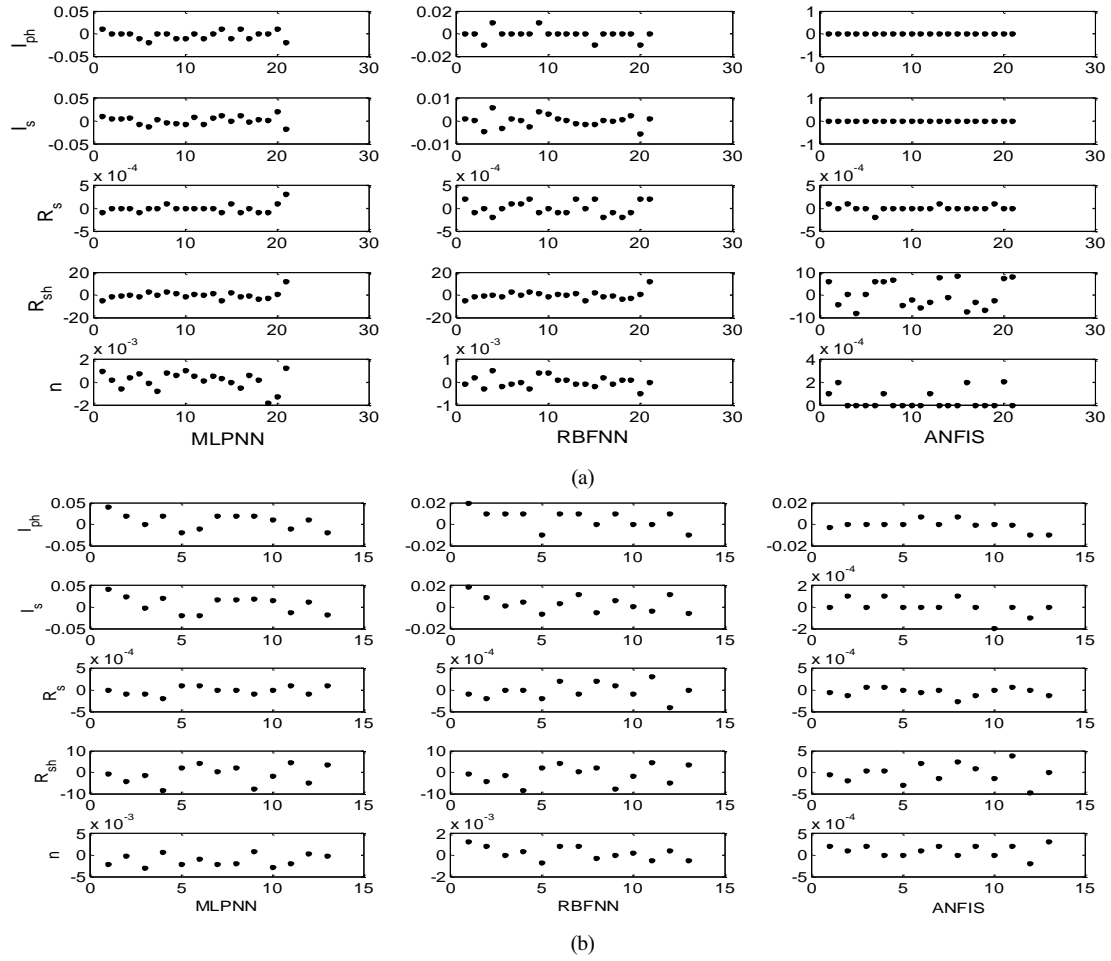


Figure 12 RMSE of (a) interpolation and (b) extrapolation, estimation by using MLPNN (2, 5, 5), RBFNN (2, 15, 5), and ANFIS([1,6], 6, 1) model for  $I_{ph}$  and  $I_s$ , ANFIS([3,4],12,1) model for  $R_s$  and  $R_{sh}$  and ANFIS([2,5],10, 1) model for  $n$ .

As seen in Fig. 12 (a) and (b), ANFIS model has shown ability in higher accuracy with lower RMSE both interpolation and extrapolation than MLPNN and RBFNN model for estimation of all parameters. MLPNN performed better than RBFNN in case of parameter  $R_s$  and  $R_{sh}$  while RBFNN performed better than MLPNN in case of the rest of parameters. The estimation results for all parameters by extinct 5 ANFIS models are shown in Fig. 13(a) and (b) for interpolation and extrapolation respectively. From the results, it can be seen that ANFIS models has high precision by providing estimation values equal to the actual value.

However, searching for high dimension of ANFIS parameter by combining of BP gradient descent and a least-squares method usually traps in the local minimum. In this work, GA is used for searching the ANFIS parameter and simultaneously optimized the ANFIS structure by reducing the number of rule to decrease computation time in the practice.

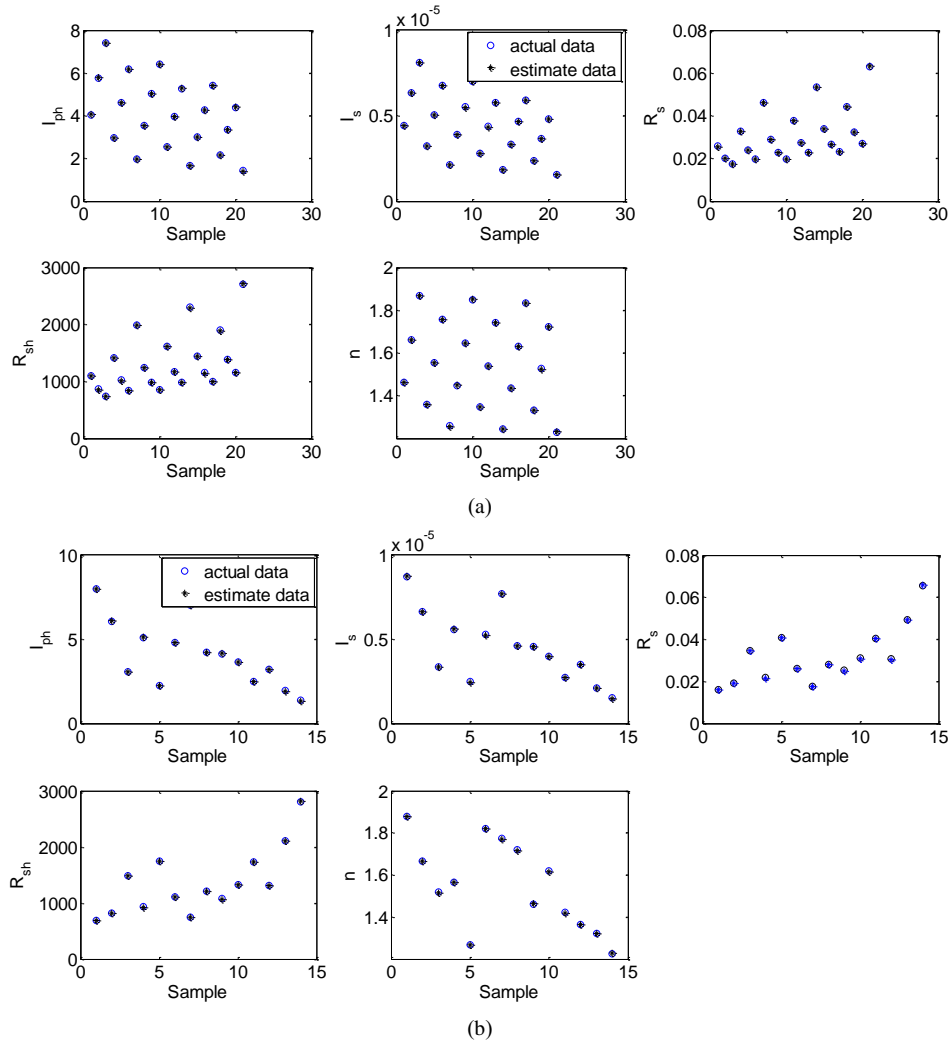


Figure 13 Estimation results by ANFIS model of all parameter for (a) interpolation and (b) extrapolation approximation.

#### 4.2 ANFIS model reduced number of rule by GA

Basically, the rule node of ANFIS is formed by the linguistic fuzzy rule *if-then* model that is self-generated by the system. As shown in the simulations in previous section, the number of rule nodes is dependent on the  $n$  number of inputs and  $m_1, m_2, \dots, m_n$  number of linguistic fuzzy sets which are generated  $m_1 \times m_2 \times \dots \times m_n$  rules by default. In the estimation, the quality of parameter accuracy depends on effectiveness of these rules. However, all the self-generated rules do not contribute enough for the accuracy improvement while increase the computation time. In this work, the redundant rules of ANFIS model are removed by GA while maintaining the accuracy in acceptable range. The selected ANFIS for each estimated parameters in previous section are taken into reducing the rule and simultaneously adjusted the parameter of the Gaussian function and consequence parameter of the significant rule. Therefore, the diagram in Fig. 9 is modified in Fig. 14.

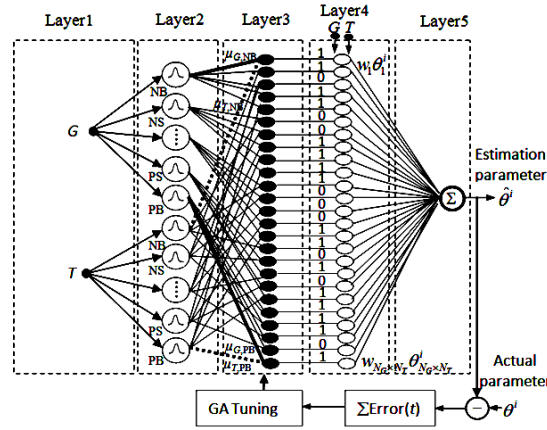


Figure 14 ANFIS architecture for estimation PV module parameters with parameter tuning by using GA.

The individual chromosome composes with genes which are represented for each parameter with the real value accept for rules which are served for the binary  $\{0, 1\}$  and shown in Fig. 14. In this work 2 input  $G$  and  $T$  has each fuzzy set  $m_1$  and  $m_2$  respectively and presented by the Gaussian function with 2 adjusted parameters,  $c$  and  $\sigma$ . The consequent parameters of each rule have 3 parameters,  $p_i$ ,  $q_i$ , and  $r_i$  according to first-order Sugeno fuzzy model. The  $m_1 \times m_2$  rules set is randomly generated in binary code which '0' means not consideration rule while '1' means takes the rule into account for calculation.

Chromosome	fuzzy set of $G$	fuzzy set of $T$	Consequence parameter	Rules
Parameter	$(C_G, \sigma_G)$	$(C_T, \sigma_T)$	$p_i, q_i, r_i$	$\{1, 0\}$
Gene	$ 1 ,  2 ,  3 , \dots,  2m_1 $	$ 1 ,  2 , \dots,  2m_2 $	$ 1 ,  2 ,  3 ,  4 , \dots,  m_1 \times m_2 \times 3 $	$ 1 ,  2 , \dots,  m_1 \times m_2 $

The GA procedure for searching of model parameter, consequence parameter of each rule and for selecting significant rule has the similar step in section 3.2. The comparison between RMSE on logarithm scale form ANFIS and ANFIS reduced rule for an interpolation and extrapolation estimation are shown in Fig. 15 (a) and (b) respectively.

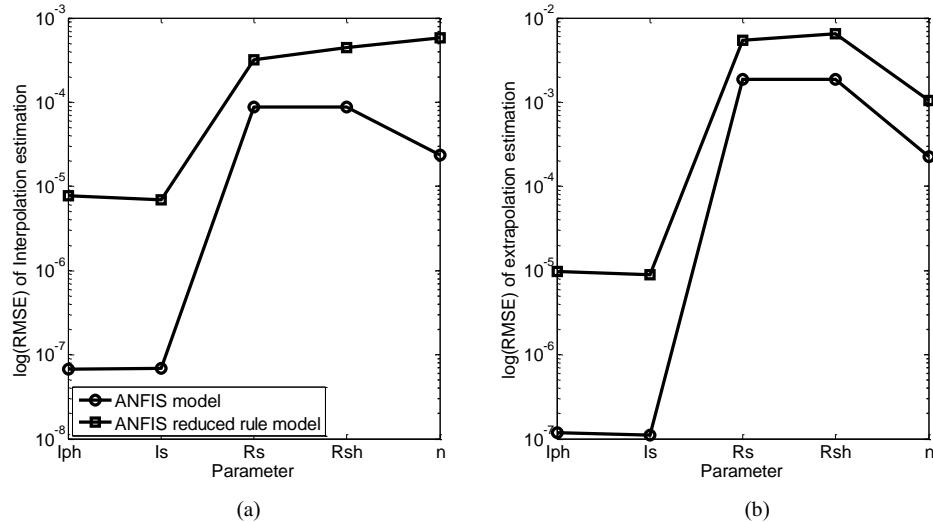


Figure 15 Comparison of RMSE between ANFIS and ANFIS reduced rule model.

The reduced rule has resulted in Table 3(a)-(c) and the number of rule is reduced by 1, 1, 7, 7, and 6 rules for parameter  $I_{ph}$  and  $I_s$ ,  $R_s$  and  $R_{sh}$ , and  $n$  respectively. The remaining parameter of this ANFIS model for parameter  $I_{ph}$ ,  $I_s$ ,  $R_s$ ,  $R_{sh}$  and  $n$  is down to 29, 29, 29, 29, and 26 respectively and collectively yields 142 parameters which is reduced by 70 parameters from the original ANFIS model.

The initial PV module parameters extracted from measured  $I$ - $V$  by GA are estimated by ANFIS reduced rule for the various weather conditions  $G$  and  $T$  to generate the  $I$ - $V$  characteristic of PV

module with the distinct of MPP for each solar irradiance and temperature are shown in Fig. 16 (a) and (b) respectively. The MPP significantly reduces with reduction of  $G$  and increment with  $T$ .

Table 3(a) Reduced rule of ANFIS model for parameter  $I_{ph}$  and  $I_s$

$\begin{matrix} T \\ \backslash \\ G \end{matrix}$	$X_{1,T}$	$X_{2,T}$	$X_{3,T}$	$X_{4,T}$	$X_{5,T}$	$X_{6,T}$
$X_{1,G}$	1	1	1	1	0	1

Table 3(b) Reduced rule of ANFIS model for parameter  $R_s$  and  $R_{sh}$

$\begin{matrix} T \\ \backslash \\ G \end{matrix}$	$X_{1,T}$	$X_{2,T}$	$X_{3,T}$	$X_{4,T}$
$X_{1,G}$	1	0	1	1
$X_{2,G}$	0	0	1	0
$X_{3,G}$	0	0	1	0

Table 3(c) Reduced rule of ANFIS model for parameter  $n$

$\begin{matrix} T \\ \backslash \\ G \end{matrix}$	$X_{1,T}$	$X_{2,T}$	$X_{3,T}$	$X_{4,T}$	$X_{5,T}$
$X_{1,G}$	1	1	0	0	1
$X_{2,G}$	0	0	1	0	0

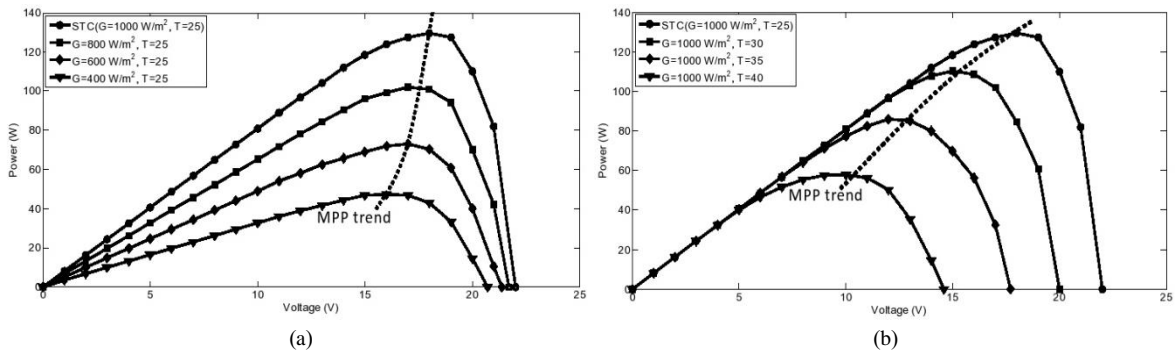


Figure 16 P-V characteristic with (a) vary on  $G$ , constant on  $T$ , (b) vary on  $T$ , constant on  $G$ .

#### 4.3 MPPT based fuzzy controller

MPPT system uses dc to dc converter to compensate the output voltage of the solar panel by keeping the voltage at the MPP. One of the most sufficient control strategies used for MPPT is the fuzzy logic controller (FLC) which controls the duty cycle ( $D$ ) of the boost converter based on the designed rules with is not mentioned here. In this work, the simulation of power control has done to test the performance of FLC with the various weather conditions which is shown by Fig. 17.

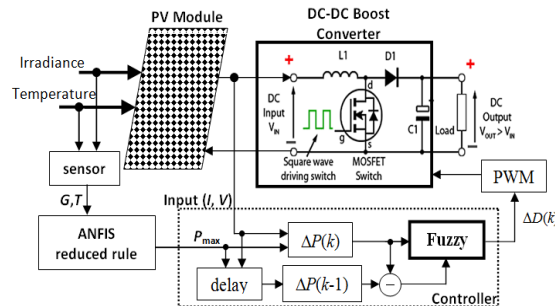


Figure 17 FLC based MPPT with the information of MPP acquired from ANFIS reduced rule model.

The implementation of ANFIS reduced rule from previous section provided the MPP at the given weather condition to set the difference of power,  $P_{max} - P_{PV}$  as the input ( $e$ ) of the FLC which simplifies the calculation. The other input of FLC is the change of power difference, ( $\Delta e$ ). The fuzzy inference is



carried out by using Mamdani method. The output of the FLC is the change of duty cycle ( $\Delta D$ ). In our proposed FLC, the derivative e.g.  $dP_{PV}/dV_{PV}$  or  $dP_{PV}/dI_{PV}$  for input variable term is disregarded to avoid the precision loss and overflow problem when dealing with the fixed-point division.

In the test, the MPP from the ANFIS reduced rule at various weather conditions ( $G, T$ ) are set from (1000, 25) to (400, 25) to (400, 30), (800, 25), (1000, 35) and to (1000, 25). FLC employs 25 rules from each 5 Gaussian membership functions of two input  $e$  and  $\Delta e$ , and also 5 Gaussian membership functions of the output  $\Delta D$ . The control result has shown in Fig. 18. At the starting point, load current and voltage, and duty ratio were set to zero. For the fast change of weather condition at second and fourth stages, the proposed FLC takes a high rise time while the slow change of weather condition at third and fifth stages, it takes a low rise time. Further, it performs stability with non-oscillation at the steady state for a low radiance better than the high radiance. The proposed FLC needs to adjust for more stable both transient and steady state. However, it successfully maintained MPP obtained from the PV module.

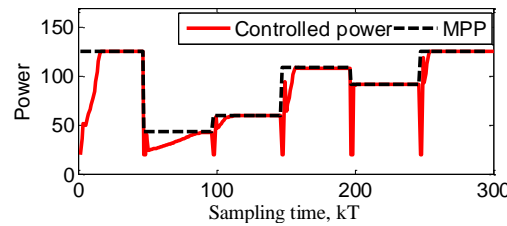


Figure 18 FLC based MPPT control effect for variety condition of PV module.

## 5. Conclusions

In this work, the measured  $I$ - $V$  data from the experiment were used to extract the equivalent circuit parameters of the PV module based single diode model at various weather conditions of irradiance and temperature by applying GA. By formulating the experimental data in a non-convex optimization problem, determination of parameters such as the photo current ( $I_{ph}$ ), the saturated diode current ( $I_s$ ), the series resistance ( $R_s$ ), the shunt resistance ( $R_{sh}$ ), and the ideality factor ( $n$ ) has shown satisfactory results by the fact that GA is capable to avoid the local minima in the non-convex optimization criteria. The preliminary solutions of these parameters are used as the train and test data for the artificial intelligence model including MLPNN, RBFNN, and ANFIS model. By the designed experiment, the structure of these models i.e. number of hidden node and number of radial basis node and the network parameter i.e. weights, biases, and rules are optimized by using RMSE as the criteria. The optimized estimation model for MLPNN and RBFNN is denoted as MLPNN(2,5,5) and RBFNN(2,15,5) respectively which has 2 similar input nodes and 5 output parameter nodes except for 5 hidden nodes for MLPNN and 15 radial basis nodes for RBFNN. While the optimized ANFIS model with 5 distinct model corresponding with 5 equivalent parameters are denoted as ANFIS([1,6],6,1) for  $I_{ph}$  and  $I_s$ , ANFIS([3,4],12,1) for  $R_s$  and  $R_{sh}$ , and ANFIS([2,5],10,1) for  $n$ . The comparison result showed that ANFIS model has the best performance and high accuracy for both interpolation and extrapolation. However, the number of network parameter of ANFIS model (212 parameters) is higher than MLPNN (45 parameters) and RBFNN (95 parameters) which is not suitable in practical implementation. GA is then used once to select the significant rule and is also adjusted the network parameter in the ANFIS model to form the ANFIS reduce rule model. ANFIS reduced rule model replaced the former one while keeping the accuracy in an acceptable level. The ANFIS reduced rule model can satisfactorily generate the  $I$ - $V$  characteristic simultaneously MPP at various weather conditions. In implementation, the MPP is used to set the difference of the power as an input for FLC based MPPT. The controller performance successfully tracked the MPP from the PV module for both slow and fast changing of weather condition.

However, the GA consumes a lot of computation time to discover the best solution. To overcome this disadvantage, the other evolutionary searching methods such as PSO, CS, SA, and etc are employed to compare with GA. In addition, in order to enhance the FLC efficiency, fuzzy cognitive networks and Takagi-Sugeno fuzzy technique may employ to improve the tracking speed and/or the parameter of the network allows the other evolutionary searching technique such as GA, PSO, CS

instead of BP to avoid local solution trapping. The hybrid technique between NNs and FL may complement each other to formulate more perfect controller of MPPT.

## References

- [1] A. Chouder, S. Silvestre, N. Sadaoui, and L. Rahmai, "Modeling and simulation of a grid connected PV system based on the evaluation of main PV module parameters," *Simul. Model Pract. Theory*, (2012) 46-58.
- [2] Available online at: [www.egco.com](http://www.egco.com) (last accessed 10/10/2015)
- [3] 2M.A. De Blas, J.L. Torres, E. Prieto, A. Garcia, "Selecting a suitable model for characterizing photovoltaic devices," *Renewable Energy*, 25 (2002) 371-380.
- [4] Y.C. Kuo, T. J. Liang, and J. Chen, "Novel maximum power point tracking controller for photovoltaic energy conversion system," *IEEE Trans. On Ind. Elect.*, 48 (3) (2001) 594-601.
- [5] R. Chenni, M. Makhoulf, T. Kerbach, and A. Bouzid, "A detailed modeling method for photovoltaic cells," *Energy*, 32(9) (2007)1724-1730.
- [6] I. Kashif, S. Zainal, T. Hamed, "Simple, fast and accurate two diode model for photovoltaic modules," *Solar Energy Mater Solar Cells*, 95(2) (2011) 586-594.
- [7] A. Jain, and A. Kapoor, "Exact analytical solution of the parameters of real solar cells using Lambert W-function," *Solar and Energy Mat. & Solar cells*, 81(2004) 269-277.
- [8] D. Picault, B. Raison, S. Bachan, J. de la Casa, and J. Aguilera, "Forecasting photovoltaic array power production subject to mismatch losses," *Solar Energy*, 84(7)(2010)1301-1309.
- [9] Y. Chen, X. Wang, D. Li, R. Hong, and H. Shen, "Parameters extraction from commercial solar cells I-V characteristics and shunt analysis," *Applied Energy*, 88(6) (2011) 2239-2244.
- [10] Y. Chen, X. Wang, D. Li, R. Hong, and H. Shen, "Parameters extraction from commercial solar cells I-V characteristics and shunt analysis," *Applied Energy*, 88(6) (2011) 2239-2244.
- [11] A. Dobos, "An improved coefficient calculator for the California energy commission 6 parameter photovoltaic module model," *J. of Solar Energy Eng.*, 134(2)(2012).
- [12] H. Tian, and et. al., " a cell-to-module-to-array detailed model for photovoltaic panels," *Solar Energy*, 86(9) (2012) 2695-2706.
- [13] K.M. El-Naggar, M.R. AlRashidi, M.F. AlHajri, and A. K. Al-Othman, "Simulated annealing algorithm for photovoltaic parameters identification," *Solar Energy*, 86 (2012) 266-274.
- [14] E.Q.B. Macabebe, C.J. Sheppard, and E.E. van Dyk, "Parameter extraction from I-V characteristics of PV devices," *Solar Energy*, 85 (2011) 12-18.
- [15] K. Ishaque, Z. Salam, S. Mkhilef, and A. Shamsudin, "Parameter extraction of solar photovoltaic modules using penalty-based differential evolution," *Appl. Energy*, 99 (2012) 297-308.
- [16] J.A. Jervase, H. Bourdouden, and A.Al-Lawati, "Solar cell parameter extraction using genetic algorithms," *Measurement Science and Tech.*, 12 (2001) 1992-1925.
- [17] M. Ye, X. Wang, and Y. Xu, "Real-time identification of optimal operating points in photovoltaic power system," *IEEE Trans. on Industrial Elect.*, 53 (2006) 1017-1026.
- [18] W. Huang, C. Jiang, L. Xue, and D. Song, "Extracting solar cell model parameters based on chaos particle swarm algorithm," in *Proc. Of the Int. Conf. on Elect. Info. and Ctrl. Eng. (ICEICE'11)*, (2011) 398-402.
- [19] I. Fister, I. Fister Jr, X.S. Yang, and J. Brest, "A comprehensive review of firefly algorithms," *Swarm and Evo. Comp.*, 2013.
- [20] M.R. Alrashidi, K.M. El-Naggar, M.F. AlHajri, and A.K. Al-Othman, "A new estimation approach for determining the I-V characteristics of solar cells," *Solar Energy*, 85(7) (2011) 1543-1550.
- [21] M.R. Alrashidi, K.M. El-Naggar, M.F. AlHajri, and A.K. Al-Othman, "Extraction of photovoltaic characteristics using simulated annealing," *Conf. on Advances in Eng. Sci. and Appl. Math.*, 2014.
- [22] H. Al-Hamadi, "Fuzzy estimation analysis of photovoltaic model parameters," *J. of Power and Energy Eng.*, 3 (2015) 39-43.
- [23] F. Bonanno, G. Capizzi, G. Napoli, and G.M. Tina, "A radial basis function neural network based approach for the electrical characteristics estimation of a photovoltaic module," *Appl. Energy*, 97 (2012) 956-961.

- [24] S. Kalika, L. Rajaji, and S. Gupta, "Intelligent technique based modeling for PVPS," *Int. J. of Eng. and Innovative Tech*, 2 (2012) 211-215.
- [25] G.Walker, "Evaluating MPPT converter topologies using a MATLAB PV model," *J. Elect. Electron. Eng. Aus.*, 21 (2001) 49-56.
- [26] L. Davis, Handbook of Genetic Algorithms, New York: Van Nostrand Reinhold, 1991.
- [27] T. Xie, H. Yu and B. Wilamowski, "Comparison between traditional neural networks and radial basis function networks," *Ind. Electron. (ISIE)*, (2011) 1194-1199.
- [28] J.K. Sing, D.K. Basu, M. Nasipuri, M. Kundu, "Improved K-means algorithm in the design of RBF neural networks," *IEEE*, 2(2003).
- [29] S. Chen, C.F.N Cowen, and P.M Grant, "Orthogonal least square learning algorithm for radial basis function networks," *IEEE Trans. On NN.*, 2(2) (1991).

Table 2 The extracted parameters of PV module at various  $G$  and  $T$  by using GA.

$G$	$T$	$I_{ph}$	$I_s \times 10^6$	$R_s$	$R_{sh}$	$n$	$G$	$T$	$I_{ph}$	$I_s \times 10^6$	$R_s$	$R_{sh}$	$n$	$G$	$T$	$I_{ph}$	$I_s \times 10^6$	$R_s$	$R_{sh}$	$n$
1000	298	8.01	8.77	0.016	690.72	1.877	875	310.5	2.8	3.07	0.035	1482.94	1.353	725	305.5	3.72	4.0693	0.0291	1247.48	1.534
1000	303	6.09	6.6652	0.019	820.68	1.667	850	298	6.81	7.455	0.019	804.688	1.858	725	310.5	2.32	2.5433	0.0412	1769.4	1.338
1000	308	4.17	4.5604	0.025	1070.6	1.463	850	303	5.17	5.665	0.022	956.096	1.65	700	298	5.61	6.139	0.0225	965.626	1.836
1000	313	2.24	2.4556	0.041	1749	1.267	850	308	3.54	3.876	0.029	1247.27	1.449	700	303	4.26	4.6656	0.0267	1147.32	1.631
975	298	7.81	8.5508	0.016	707.35	1.874	850	310.5	2.72	2.982	0.036	1523.88	1.351	700	305.5	3.59	3.929	0.0301	1289.26	1.531
975	303	5.94	6.4986	0.02	840.45	1.664	825	298	6.61	7.235	0.019	827.573	1.855	700	310.5	2.24	2.4556	0.0426	1828.65	1.335
975	308	4.06	4.4464	0.026	1096.4	1.461	825	303	5.02	5.499	0.023	983.287	1.647	675	298	5.41	5.9198	0.0233	999.157	1.832
975	313	2.19	2.3942	0.042	1791.1	1.265	825	308	3.44	3.762	0.03	1282.74	1.447	675	303	4.11	4.499	0.0277	1187.16	1.627
950	298	7.61	8.3315	0.017	724.84	1.871	825	310.5	2.64	2.894	0.037	1567.22	1.349	675	305.5	3.46	3.7886	0.0311	1334.03	1.527
950	303	5.78	6.3319	0.02	861.22	1.661	800	298	6.41	7.016	0.02	851.84	1.851	675	310.5	2.16	2.3679	0.0441	1892.15	1.332
950	308	3.96	4.3324	0.026	1123.5	1.459	800	303	4.87	5.332	0.024	1012.12	1.644	650	298	5.21	5.7005	0.0241	1035.18	1.828
950	313	2.13	2.3328	0.043	1835.4	1.263	800	308	3.33	3.648	0.031	1320.35	1.444	650	303	3.96	4.3324	0.0287	1229.96	1.624
925	298	7.41	8.1123	0.017	743.23	1.868	800	310.5	2.56	2.806	0.038	1613.17	1.346	650	305.5	3.33	3.6483	0.0322	1382.13	1.524
925	303	5.63	6.1653	0.021	883.08	1.659	775	298	6.21	6.797	0.02	877.621	1.848	650	310.5	2.08	2.2802	0.0457	1960.37	1.329
925	308	3.85	4.2184	0.027	1152	1.457	775	303	4.72	5.166	0.024	1042.75	1.641	625	298	5.01	5.4813	0.025	1073.99	1.824
925	313	2.07	2.2714	0.044	1882	1.261	775	308	3.23	3.534	0.032	1360.31	1.441	625	303	3.8	4.1658	0.0297	1276.07	1.62
900	298	7.21	7.893	0.018	762.62	1.865	775	310.5	2.48	2.719	0.039	1662	1.343	625	305.5	3.2	3.508	0.0334	1433.94	1.52
900	303	5.48	5.9987	0.021	906.11	1.656	750	298	6.01	6.578	0.021	905.063	1.844	625	310.5	2	2.1925	0.0474	2033.86	1.326
900	308	3.75	4.1044	0.028	1182.1	1.454	750	303	4.57	4.999	0.025	1075.36	1.638	600	298	4.81	5.262	0.026	1115.92	1.819
900	313	2.02	2.21	0.045	1931.1	1.259	750	308	3.12	3.42	0.033	1402.85	1.438	600	303	3.65	3.9991	0.0309	1325.88	1.616
875	298	7.01	7.6738	0.018	783.07	1.862	750	310.5	2.4	2.631	0.04	1713.96	1.341	600	305.5	3.08	3.3677	0.0347	1489.92	1.516
875	303	5.33	5.8321	0.022	930.41	1.653	725	298	5.81	6.358	0.022	934.335	1.84	600	310.5	1.92	2.1048	0.0493	2113.27	1.322
875	308	3.64	3.9904	0.028	1213.8	1.452	725	303	4.41	4.832	0.026	1110.14	1.634							